International Journal of Fluid Mechanics & Thermal Sciences
2015; 1(3): 72-82
Published online February 26, 2016 (http://www.sciencepublishinggroup.com/j/ijfmts)
doi: 10.11648/j.ijfmts.20150103.15
ISSN: 2469-8105 (Print); ISSN: 2469-8113 (Online)

Heat and Mass Transfer in 3D Inclined Lid-Driven Solar Distiller

Lioua Kolsi[1, 2]

[1]Mechanical Engineering Department, College of Engineering, Haïl University, Haïl City, Saudi Arabia
[2]Research Unit of Metrology and Energy Systems, National Engineering School, Energy Engineering Department, University of Monastir, Monastir City, Tunisia

Email address:
lioua_enim@yahoo.fr

To cite this article:
Lioua Kolsi. Heat and Mass Transfer in 3D Inclined Lid-Driven Solar Distiller. *International Journal of Fluid Mechanics & Thermal Sciences.* Vol. 1, No. 3, 2015, pp. 72-82. doi: 10.11648/j.ijfmts.20150103.15

Abstract: This work is dedicated to study numerically an inclined solar distiller subject of a moving cold wall. The cavity is heated from left side and cooled from the right one. Constant and different concentrations are imposed in the two vertical sides of the cavity, while the other walls are adiabatic and impermeable. The flow is considered laminar and caused by the interaction of the thermal energy and the chemical species diffusions. Equations of concentration, energy and momentum are formulated using vector potential-vorticity formulations in its three-dimensional form, then discretized by the finite volumes method. The Rayleigh, Prandtl, Lewis numbers and buoyancy ratio are respectively fixed at $Ra=10^5$, Pr=0.7, Le=0.85 and N=0.85. Reynolds number (Re) is varied along the study from 0 to 150. The angles for the cavity inclination under this investigation are considered to be 0°, 30°, 45°, 60° and 90°. A particular interest to the flow structure and evolution of the heat and transfer i highlight in this paper.

Keywords: Lid Driven, Solar Distiller, Heat and Mass Transfer, Flow Structure

1. Introduction

Improving the performance of a solar still remains a concern for all designers and producers. In fact, solar distillation is the best way to produce potable water from brackish and underground water at low cost especially for the arid and semi-arid regions. Such an improvement requires optimization between technical performance and cost. In this study, big interest is reserved to simulate heat and mass transfer in an inclined cavity subject of a moving cold wall. This case of configuration is widely used in many industrial applications and needs more detailed information's. Both buoyancy-induced and lid-driven flows inside an enclosure are often encountered in many engineering applications as the nuclear reactors, lubricating grooves, coating and industrial processes, float glass manufacturing and food industries. Many researchers studied the double diffusive convection in its two and three dimensional forms, numerically and experimentally. Also, many authors are interested to study the case of cavity with a moved wall.

In this work, we focus our interest to study numerically an inclined solar distiller characterized by two verticals walls subject of different and opposite gradients of temperature and concentration. The hot wall warms up by the solar radiation inducing the evaporation of a water film; the vapor thus produced mixes with the air then condenses when it reaches the cold wall. The cold wall (in which the condensation takes place) is moved at a varied velocity and this via a photovoltaic installation. The hot wall (in which the evaporation of the brackish water occurs) is fixed and it is at high concentration. In this study, big interest is reserved to simulate heat and mass transfer through the solar distiller and especially between the two vertical films of condensation and evaporation. This case of configuration is widely used in many industrial applications and needs more detailed information's. Both buoyancy-induced and lid-driven flows inside an enclosure are often encountered in many engineering applications as nuclear reactors, lubricating grooves, coating, industrial processes, float glass manufacturing and food industries. Many researchers studied numerically and experimentally, the double diffusive convection in two and three-dimensional configurations,. Also, many authors were interested to study the case of cavity with a moved wall.

Gobin and Bennacer [1] studied numerically the double diffusive natural convection in a two dimensional cavity filled with a binary fluid and subject of horizontal temperature and concentration gradients with cooperating volume forces. They showed that for a high number of Lewis, the thermal transfer goes down as the buoyancy ratio increase. Lee and Hyun [2] and Hyun and Lee [3] have reported numerical solutions for double-diffusive convection in a rectangular enclosure with aiding and opposing temperature and concentration gradients. Their solutions were compared favorably with reported experimental results. The performance of a solar distiller could be ameliorate by many parameters such as depth of water, glass cover angle, fabrication materials, temperature of water in the basin and insulation thickness, etc. In fact, with the aim to maximize the distillate productivity of the apparatus over current solar stills, Naim et al [4] developed a single-stage solar desalination spirally-wound module of original design that makes use of both the latent heat of condensation of the formed vapor and the sensible heat of the concentrated solution, in preheating the incoming saline water. For the solar desalination of brackish water, the most used technology is the capillary film distiller which is composed of identical cells of evaporation-condensation Bouchekima et al. [5, 6 and 7]. Ben Snoussi et al. [8] studied this configuration by simulating numerically the natural convection in 2D rectangular cavities. Results show that the flow, mass and thermal fields are strongly dependent on Rayleigh number and aspect ratio. A recent detailed review on active solar distillation procedures and modeling can be found in the work of Sampathkumar et al. [9]. The three-dimensional configuration wasn't widely studied numerically. In fact, Bergeon and Knobloch [10] studied bifurcations in the double diffusive convection in three dimensional cavity subjected to horizontal temperature and concentration gradients. They've proved that in certain conditions, the flow is unstable and the rate is periodic. Indeed, the mechanism responsible for these oscillations is identified and the oscillations turned up to be an indirect consequence of the presence of a bifurcation to the longitudinal structures of the three dimensional flow which do not exists in a two dimensional formulation. Sezai and Mohamad [11] have demonstrated that, in case of a cube-shaped cavity, the structure of the flow of the thermo-solutal natural convection, in the opposite case for values of buoyancy number superior to the unit, is purely three dimensional for certain values of the used parameters such as the buoyancy forces, the thermal Rayleigh and the Lewis numbers. The same configuration was studied by Abidi et al. [12] but with heat and mass diffusive horizontal walls. They mentioned that the effect of the heat and mass diffusive walls is found to reduce the transverse velocity for the thermal buoyancy-dominated regime and to increase it considerably for the compositional buoyancy-dominated regime.

Ghachem et al. [13] studied numerically the double diffusive natural convection and entropy generation in three-dimensional solar dryer with an aspect ratio equal to 2. They found that the variation of the buoyancy ratio affects significantly the isotherms distributions, iso-concentrations and the flow structure. Particularly for N=1, the flow is completely three-dimensional. Besides, they found that all kinds of entropies generation present a minimum for N=1. This result is due to the competition between thermal and compositional forces. These entropies rise considerably when N grows. On the one hand, the maximum of Bejan number is found for N=1 witch indicated the domination of heat and mass irreversibilities. Outside, friction irreversibilties are largely dominant. On the other hand, distribution of Local Nusselt numbers changes with changing buoyancy ratio and take a complex structure for N=1. Lid-driven flow carries the interest of many industrial applications such as electronic cards cooling, crystal growth, building insulation high performance, multi-screen structures used for nuclear reactors, food processing, production of float glass, solar collectors, oven drying, etc.

Many authors were interested to study the flow structure behavior. Moallemi and Jang [14] conducted a numerical investigation to analyze the effect of Prandtl number on the flow structure and heat transfer in a bottom heated lid-driven square cavity. These authors found that the influence of buoyancy on the flow and heat transfer was more pronounced for higher values of *Pr*, if *Re* and *Gr* were kept constant. They found also that the natural convection effects were always assisting the forced convection heat transfer, and the extent of the contribution was a function of *Pr* and *Ri*. Sharif [15] studied numerically the 2D laminar mixed convection in a rectangular enclosure with an aspect ratio equal to 10 and subject of a top moving hot wall. Computations are performed for Rayleigh numbers ranging from 10^5 to 10^7 keeping the Reynolds number fixed at *408.21*, thus encompassing the dominating forced convection, mixed convection, and dominating natural convection flow regimes. The Prandtl number is taken as *6* representing water. The author studied the effects of inclination of the cavity on the flow and thermal fields for inclination angles ranging from *0°* to *30°*. He found that the average Nusselt number increases with cavity inclination. The author concluded that the average Nusselt number increases mildly with cavity inclination for the dominant forced convection case dictated by *Ri=0.1*. In contrast, it increases much more rapidly with inclination for the other dominant natural convection case dictated by *Ri=10*. He found also that the local Nusselt number at the heated moving lid starts with a high value and decreases rapidly and monotonically to a small value towards the right side. Numerical simulation of unsteady mixed convection in a driven cavity using an externally excited sliding lid has been studied by Khanafer et al. [16]. These authors examined the fluid flow and heat transfer characteristics in the range of Reynolds number, Grashof number, and the dimensionless lid oscillation frequency (x) such that: $10^2 \leq Re \leq 10^3$, $10^2 \leq Gr \leq 10^5$, and $0.1 \leq x \leq 5$. They found the energy transport process and drag force behavior depending on the conduct of the velocity cycle would either enhance or retard by the Reynolds number and

Grashof number.

Oztop et al. [17] studied numerically the conjugate heat transfer by mixed convection and conduction in lid-driven enclosures with thick bottom wall. The enclosure is assumed to be heated isothermally from the bottom. The temperature of the top moving wall, which has constant speed, is lower than that of the outside of bottom wall. Vertical walls of the enclosure are adiabatic. Governing parameters are solved for a wide range of Richardson numbers, ratio of height of bottom wall to enclosure height and thermal conductivity ratio. The fluid flow and heat transfer induced by the combined effects of the driven lid and the buoyancy force within rectangular enclosures were investigated by Waheed [18]. Investigation for various Prandtl number, Richardson number, and aspect ratio at a Reynolds number of *100* was performed by this author. The results showed fluid flow and energy distributions within the enclosures and heat flux on the heated wall are enhanced by the increase in the Richardson number. Sivakumar et al. [19] conducted analysis of the mixed convection heat transfer in lid-driven cavities with different lengths of the heating portion at different locations. Results showed that the heat transfer rate is enhanced on reducing the heating portion provided the portion is at middle or top of the hot wall of the cavity. Cheng [20] studied the flow and heat transfer in a 2-D square cavity where the flow is induced by a shear force resulting from the motion of the upper lid combined with buoyancy force due to bottom heating. The two vertical walls of the cavity are adiabatic while the top moving-wall and the bottom wall are maintained isothermally but the temperature of the bottom wall is higher than that of the top moving-wall. A sudden drop of Nusselt number is observed by the author at *Re=713, 376, 248, 129,* and *61* for *Ri=0.5, 1, 2, 10,* and *100*, respectively, due to the change of flow and thermal structures, heat transfer mechanism, and kinetic energy. Cheng [14] concluded that there is no bifurcation that occurred for the ranges of *Re* (*10≤Re≤2200*) and *Pr* (*Pr=0.01, 0.71, 6.0*, and *50*) studied when the flow is dominated by the forced convection (*Ri=0.01*). However, when *Ri=1* and *10*, the flows undergoes a bifurcation for certain Reynolds number which is a function of the fluid Prandtl number. Laminar mixed-convection in a lid-driven square cavity having an isothermally heated square internal blockage has been investigated numerically by Akand et al. [21]. Central and eccentric placement of the blockage inside the cavity is considered in this investigation. Authors found that for any size of the blockage placed anywhere in the cavity, the average Nusselt number does not change much with increasing Richardson number until the Richardson number approaches the value of the order of *1* due to dominating forced convection. In other hand, when the Richardson number is increased beyond *1* (*Ri ≥ 1*), the flow regime is natural convection dominated and the *Nu* increases monotonically with *Ri*. However, the scale of increase of the Nu varies much with the blockage size.

Hajri et al. [22] studied numerically the steady and two-dimensional double-diffusive natural convection in a triangular cavity. This configuration is encountered in greenhouse solar stills where vertical temperature and concentration gradients between the saline water and transparent cover induce flows in a confined space. They found that for small values of the buoyancy ratio and the Lewis number, there is a little increase in the heat and mass transfer over that due to conduction. For the higher values, the convective mode dominates. Alvarado-Juárez et al. [23] studied numerically a conjugate heat and mass transfer in a solar still device. They studied the conservation of mass, momentum, energy and concentration of water vapor equations for laminar natural convection and surface thermal radiation in an inclined cavity. The authors found that the average convective Nusselt number and Sherwood number increase about 25% and 15% respectively when surface thermal radiation is considered, as a consequence, the total Nusselt number increases about 175%. Also, they proved that the Nusselt number increases as the tilted angle or Ra number increases and decreases as the aspect ratio decreases. Indeed, the distillate mass flow rate increases as the tilted, Rayleigh number or aspect ratio increases.

Experiments and numerical simulation have been performed by Mohamed and Viskanta [24] to investigate natural and mixed convection in a shallow rectangular cavity filled with liquid gallium. The cavity was heated from below and cooled from above either in the absence or presence of lid motion. The authors conducted experiments in a cavity having aspect ratios of *10* and *5* in the longitudinal and span-wise directions, respectively. They have performed also a three dimensional unsteady direct numerical simulations to obtain improved understanding of the flow structure in the cavity. The results show that lid motion has a significant effect on the flow and thermal structures in the cavity. For Richardson numbers less than unity, the effect of the lid motion is to reorganize the flow and to make the flow structure quasi-two-dimensional.

Ouertatani et al. [25] have investigated a three-dimensional laminar mixed convection in a double lid-driven cubic cavity filled with air (*Pr=0.71*) for suitable combinations of three different Reynolds numbers and three different Richardson numbers. They studied the effects of varying both Reynolds and Richardson numbers on the resulting convection. Their results show that when large *Ri* is united with low *Re*, two primary vortex are observed circumscribed in the proximity of the two moving lids and their intensity is slightly modified when *Ri* decreased. When *Ri* is small and *Re* is large, three-dimensionalities of the isotherm patterns are manifested. Kolsi et al. [26] examined laminar mixed convection and entropy generation in a cubic lid-driven cavity numerically. In their study left side of cavity moved in y direction, and the cavity was heated from left side and was cooled from right while other surfaces were adiabatic. They found direction of lid motion is an effective parameter on both entropy generation and heat and fluid flow for low values of Richardson number, but is irrelevant at high Richardson number.

Hsiao [29] performed an analysis for heat and mass

transfer of a steady laminar boundary-layer flow of an electrically magnetic conducting fluid of second-grade subject to suction and to a transverse uniform magnetic and electric field past a semi-infinite stretching sheet. In this work the author considered the mass transfer phenomena to a coupled heat and mass transfer boundary-layer equations. Lin and Hsiao [30] studied the energy conversion conjugate conduction convection Ohmic mixed heat and mass transfer of an incompressible viscoelastic fluid on thermal forming stretching sheet using the similarity transformation method to change the partial differential equations transform to a set of nonlinear ordinary differential equations, and it has also been used an implicit finite-difference method to solve the system's equations. The numerical calculating results for the conjugate heat transfer energy conversion problem have been carried out as function of several parameters

This numerical study investigates the heat and mass transfer and the structure of flow induced by double diffusive convection in a three-dimensional inclined solar distiller with moving cold wall. The results are divided into three parts. The first one is reserved to the study of a vertical cavity subject of moved cold wall. The second part is devoted to study the effect of the cavity inclination angle and Reynolds numbers. This case is helpful to pick to major modifications and effects of the heat and mass transfer and flow structure in a solar distiller. Finally, a study of the variation of Nusselt number is presented in order to localize the regions where the maximum and minimum of heat exchange occurs.

2. Definition of the Physical Model

The geometry under consideration (figure 1) is a square basic parallelepipedic enclosure (side L), with aspect ratios Ay=H/W=2 and Az=L/W=2. The vertical hot wall warms up by the solar radiation inducing the evaporation of water film. The vapor thus produced mixes with the air then condenses when it reaches the cold moved wall. As it said above this study is focused especially to the mixed part between the two thin films. For this, the cavity is filled with an ideal binary mixture of a solvent vapor and a non-condensable gas, characterized by a number of Prandtl equal to 0.7 and a number of Lewis equal to 0.85 (for more details see Ghachem et al. [13]). Different temperatures and concentrations are specified between the left (T'_h, C'_h) and right vertical walls (T'_C, C'_l), and zero heat and mass fluxes are imposed (Fig. 1). Right side moves in vertical ways. The flow is assumed to be laminar and the binary fluid is assumed to be Newtonian and incompressible. The physical properties of the fluid are supposed to be constant and the Boussinesq approximation is adopted. Finally, the Soret and Dufour effects are assumed to be negligible.

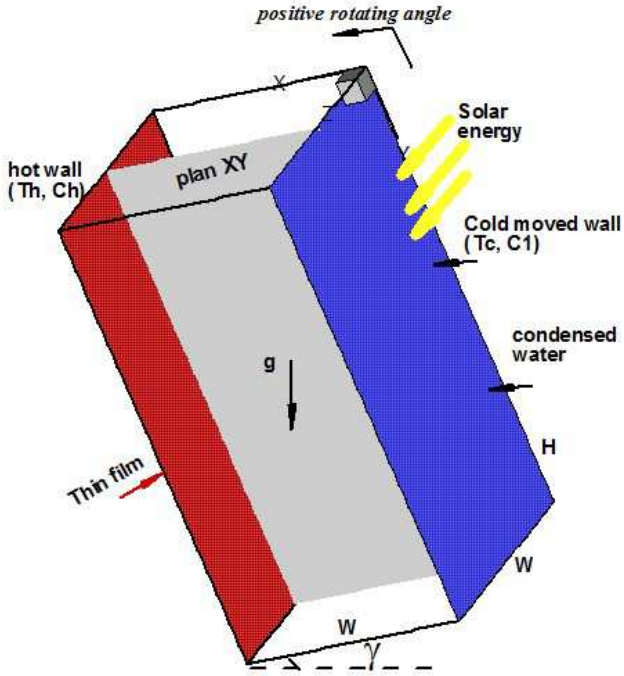

Figure 1. *Physical models.*

3. Governing Equations and Numerical Solution

In order to eliminate the pressure term, which is delicate to treat, the numerical method used in this work is based on the vorticity vector potential Formalism $(\vec{\psi}-\vec{\omega})$ which are respectively defined by the two following relations:

$$\vec{\omega}' = \vec{\nabla}\times\vec{u}' \text{ and } \vec{u}' = \vec{\nabla}\times\vec{\psi}' \tag{1}$$

The equation setting and numerical method are described with more details in the article of Ghachem et al. [13]

After non-dimensionalizing the system of equations controlling the phenomenon is:

$$-\vec{\omega} = \nabla^2\vec{\psi} \tag{2}$$

$$\frac{\partial\vec{\omega}}{\partial t} + (\vec{u}.\nabla)\vec{\omega} - (\vec{\omega}.\nabla)\vec{u} = \Delta\vec{\omega} + Ra.\Pr.\begin{bmatrix} (\frac{\partial T}{\partial z} + N\frac{\partial C}{\partial z})\cos\gamma \\ (-\frac{\partial T}{\partial z} - N\frac{\partial C}{\partial z})\sin\gamma \\ ((-\frac{\partial T}{\partial x}\cos\gamma + \frac{\partial T}{\partial y}\sin\gamma) + N(-\cos\gamma\frac{\partial C}{\partial x} + \sin\gamma\frac{\partial C}{\partial y})) \end{bmatrix} \tag{3}$$

$$\frac{\partial T}{\partial t} + \vec{u}.\nabla T = \nabla^2 T \tag{4}$$

$$\frac{\partial C}{\partial t} + \vec{u}.\vec{\nabla}C = \frac{1}{Le}\vec{\nabla}^2 C \tag{5}$$

With:

$N = \frac{\beta_c (C_h - C_l)}{\beta_T (T_h - T_C)}$; $Ra = \frac{g \beta_T (T_h - T_C) L^3}{\nu . \alpha}$; $\Pr = \frac{\nu}{\alpha}$ and $Le = \frac{\alpha}{D}$

The Richardson is defined as: $Ri = \frac{Gr}{\mathrm{Re}^2} = \frac{Ra}{\Pr . \mathrm{Re}^2}$

The control volume finite difference method is used to discretize equations (2)-(5). The central-difference scheme for treating convective terms and the fully implicit procedure to discretize the temporal derivatives are retained. The grid is uniform in all directions with additional nodes on boundaries. The successive relaxation iterating scheme is used to solve the resulting non-linear algebraic equations. The time step 10^{-4} and spatial mesh 51x101x101are retained to carry out all numerical tests. The solution is considered acceptable when the following convergence criterion is satisfied for each step of time:

$$\sum_{i}^{1,2,3} \frac{\max \left| \psi_i^n - \psi_i^{n-1} \right|}{\max \left| \psi_i^n \right|} + \max \left| T_i^n - T_i^{n-1} \right| \le 10^{-5} \qquad (6)$$

Boundary conditions for considered model are given as follows:

- Temperature:

$T = 1$ at $x = 0$, $T = 0$ for $x = 1$

$\frac{\partial T}{\partial n} = 0$ on all walls (adiabatic).

- Concentration

$C = 1$ at $x = 0$, $C = 0$ for $x = 1$

$\frac{\partial C}{\partial n} = 0$ on all walls (impermeable).

- Vorticity

$\omega_x = 0$, $\omega_y = -\frac{\partial u_3}{\partial x}$, $\omega_z = \frac{\partial u_2}{\partial x}$ at $x = 0$ and 1

$\omega_x = \frac{\partial u_3}{\partial y}$, $\omega_y = 0$, $\omega_z = -\frac{\partial u_1}{\partial y}$ at $y = 0$ and 1

$\omega_x = -\frac{\partial u_2}{\partial z}$, $\omega_y = \frac{\partial u_1}{\partial z}$, $\omega_z = 0$ at $z = 0$ and 1

- Vector potential

$\frac{\partial \psi_x}{\partial x} = \psi_y = \psi_z = 0$ at $x = 0$ and 1

$\psi_x = \frac{\partial \psi_y}{\partial y} = \psi_z = 0$ at $y = 0$ and 1

$\psi_x = \psi_y = \frac{\partial \psi_z}{\partial z} = 0$ at $z = 0$ and 1

- Velocity

$u_1 = u_2 = u_3 = 0$ at x=1, y=0, y=1, z=0 and z=1 $u_1 = u_3 = 0$ and $u_2 = \mathrm{Re}.\Pr$ at x=0

Local and average Nusselt is given as follows

$$Nu = \left. \frac{\partial T}{\partial x} \right|_{x=0,1}, \quad Nu_m = \int_0^1 \int_0^1 Nu . \partial y . \partial z \qquad (7)$$

Local and average Sherwood is given as follows

$$Sh = \left. \frac{\partial C}{\partial x} \right|_{x=0,1}, \quad Sh_m = \int_0^1 \int_0^1 Sh . \partial y . \partial z \qquad (8)$$

4. Validation and Grid Dependency

Several girds were tested to perform the grid dependency. Table.1 shows that a grid of size 51x51x51 is satisfying for this study. Checks were conducted to validate the calculation procedure by performing simulation for double-diffusive convection flow in a vertical rectangular enclosure, which combined horizontal temperature and concentration gradients effects. For this, the validation of the present numerical solution is done by making comparisons of the isotherm, concentration, z-vector potential and streamlines contours of the present work, with those of Nishimura et al. [27]. Figures 2 and 3 show the isotherms, isoconcentration, z-vector potential and velocity projection in the XY-plan for N=0.8 and N=1.3. Our results are in good agreement with those of Nishimura et al. [27]. It is noted that in the 3D configurations the contours of the streamlines are not closed compared with the 2D configurations. The code is also validated against the results of Chamkha et al. [28] (Table 2) and a quasi-perfect concordance is noticed.

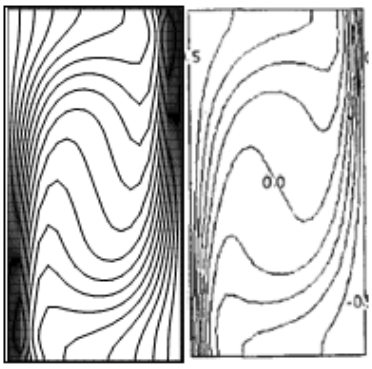

T

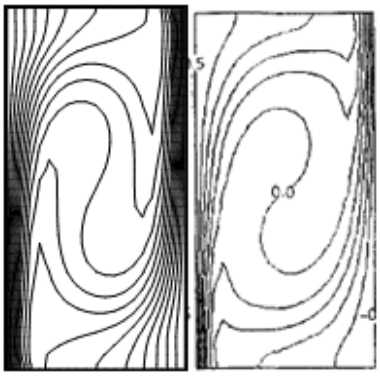

C

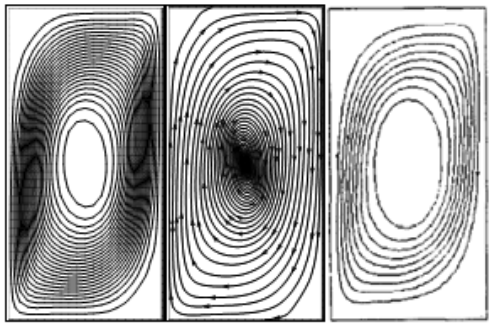

ψ_z and Velocity projection.

Figure 2. *Plots of isotherms, isoconcentration, z-vector potential and velocity projection in the XY-plan for N=0.8. (Prsent results (left) and those of Nishimura et al. [27] (right)).*

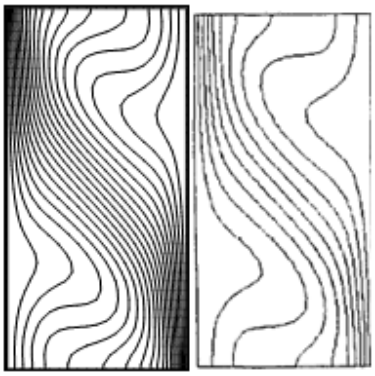

T

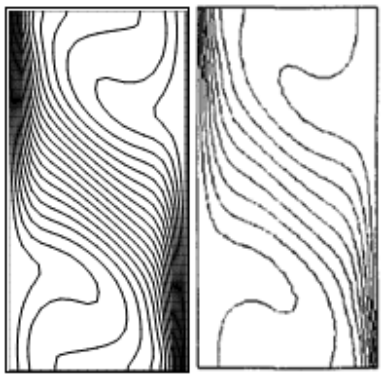

C

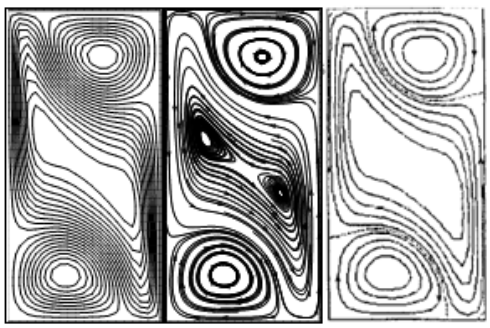

ψ_z and Velocity projection.

Figure 3. *Plots of isotherms, isoconcentration, z-vector potential and velocity projection in the XY-plan for N=1.3 (Present results (left) and those of Nishimura et al. [27] (right)).*

Table 1. *Grid dependency for ($Ra=10^5$, Re=40, Le=0.85, Pr=0.7 and N=0.85).*

Grid	31x31x31	41x41x41	51x51x51	61x61x61
$\overline{Nu}$	7.014	7.111	7.232	7.239

Table 2. *Comparison between the present results and literature for ($Ra=10^5$, Pr=1, Le=2 and N=1).*

Ha	Authors	$\overline{Nu}$	$\overline{Sh}$
0	Present result (Chamkha et al. [28])	3,358 (3,319)	4,078 (4,030)
5	Present result (Chamkha et al. [28])	3,247 (3,215)	3,948 (3,909)
10	Present result (Chamkha et al. [28])	3,093 (3,048)	3,853 (3,797)
15	Present result (Chamkha et al. [28])	2,905 (2,868)	3,792 (3,744)
20	Present result (Chamkha et al. [28])	2,539 (2,497)	3,714 (3,652)

5. Results and Discussions

The flow, heat and mass transfer characteristics are governed by the dimensionless parameters Re, Gr, Le, Pr and N. The Richardson number, Ri = Gr/Re2, measures the importance of buoyancy-driven natural convection relative to lid-driven forced convection. It may be noted that the buoyancy force ratio, N, is fixed at -0.85 which characterizes pure thermal regime. In this study, Prandtl and Lewis numbers are fixed respectively at 0.7 and 0.85 corresponding to air-vapor mixture properties.

5.1. Effect of the Variation of the Re for a Vertical Cavity

Figure 4 shows the variation of the flow structure when Re is varied from 0 to 150. For Re=0, the flow is characterized by one central cell turning in the clockwise. By increasing Re (from 20 to 60), the central cell is divided into two vortex which become more and more developed and stretched to the down part of the moved wall. For Re=100, the left vortex (near the hot wall) keeps its place however the other vortex is moved parallel to the down part of the cold moved wall. These vortexes become L-shaped. When Re reaches a value of 150, the flow returns to a mono-cellular structure and the vortex becomes closer to the down corner of the moved cold wall.

Figures 5 and 6, show respectively the iso-surfaces of temperature and concentration. The profiles iso-surfaces of temperature and iso-surfaces concentration are similar due to value of Lewis nimber which is near to 1. These iso-surfaces present a horizontal stratification in terms of the increase of Re number. Nevertheless, the stepper gradient of temperature (or concentration) is more and more pronounced when the Re number increase.

When the thermal (solutal) gradients are tighter, the heat (mass) transfer is more intense. In the one hand, the movement of the cold wall induces an acceleration of heat and mass transfer. In the second hand, it provides more homogeneous to heat and mass distribution throughout the solar distiller.

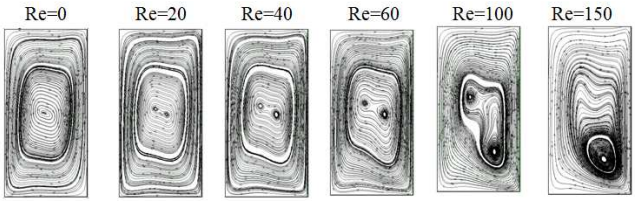

Figure 4. *Velocity vector projection in the XY-plan for γ=0 and different Re.*

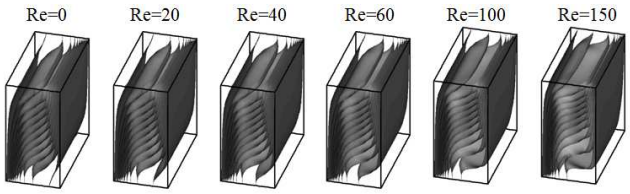

Figure 5. *Iso-surfaces of temperature for γ=0 and different Re.*

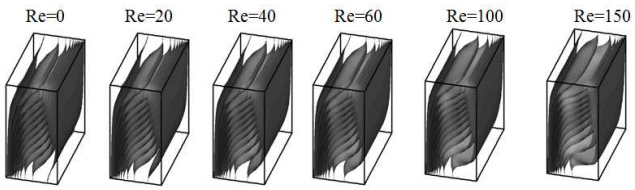

Figure 6. *Iso-surfaces of concentrations for γ=0 and different Re.*

5.2. Effect of the Inclination Angle

In this part, we present the effect of the inclination of the cavity when the cold wall is moved. These results give an idea about the evolution of heat and mass transfer all over the cavity which will be helpful to promote the heat and mass transfer in a solar distiller.

- Case 1: Re=0

Figure 7, presents the flow structure for different inclination angles. Vertical cavity (γ=0°) is taken as reference. Increasing the angle of inclination keeps the flow structure with one vortex. Thereof, is stretched to the left diagonal of the cavity when the inclination angle is equal to 30°, almost centered in the middle for (γ=45° and 60°) and slightly stretched to the right diagonal of the cavity when (γ=75°). For (γ=90°), this central vortex is moved to the top part of the cavity.

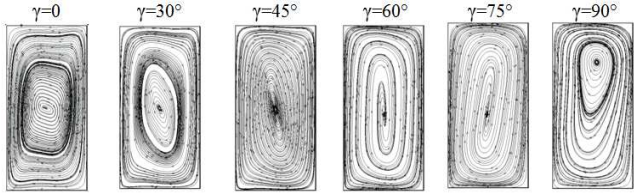

Figure 7. *Velocity vector projection in the XY-plan for Re=0 and different γ.*

Figures 8 and 9, show the iso-surfaces of temperature and concentration for Re=0 and different inclination angles. These figures show the maintaining of the vertical stratification for an inclination equal to 0°, 30° and 45°. When the inclination angle reaches a value of 60°, these iso-surfaces show a distortion especially at the upper part of the cavity. For these values of inclination angle, iso-surfaces are more linked and parallel to the fixed cold wall.

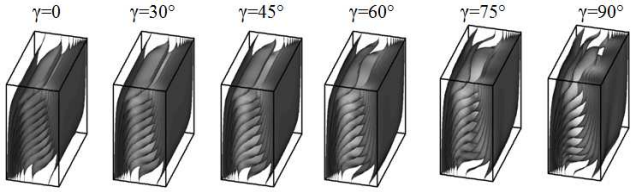

Figure 8. *Iso-surfaces of temperature for Re=0 and different (γ).*

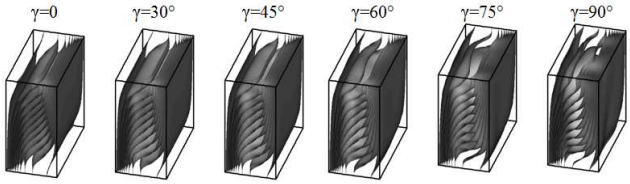

Figure 9. *Iso-surfaces of concentrations for Re=0 and different (γ).*

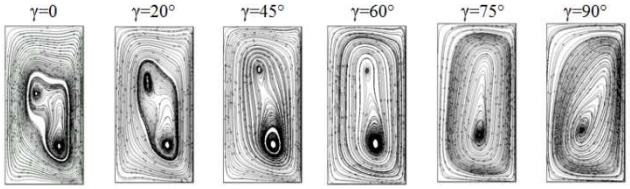

Figure 10. *Velocity vector projection in the XY-plan for Re=100 and different γ.*

- Case 2: Re=100

Figure 10 shows the projection velocity vectors in the central plan for six inclination angles (0°, 20°, 45°, 60°, 75° and 90°). The two vortex in L shaped, which appear for γ=0°, start a gradually coalition by increasing the inclination angle. In fact, the upper vortex shrinks in volume progressively from γ=20° to γ=60° and disappears for γ=75° and 90°. For this angle (γ=90°), the streamlines are more oriented towards the moved wall while they were instead diverted to the mobile wall for γ=20°.

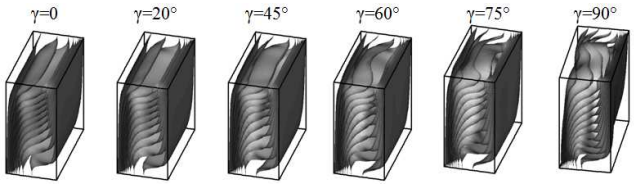

Figure 11. *Iso-surfaces of temperature for Re=100 and different (γ).*

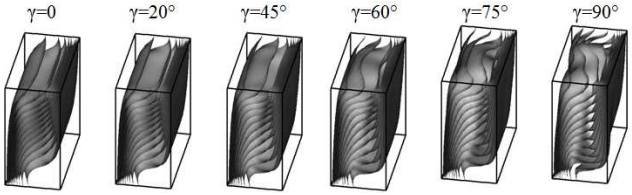

Figure 12. *Iso-surfaces of concentrations for Re=100 and different (γ).*

Figures 11 and 12, present the iso-surfaces of temperature and concentration for Re=100. As it was noted for Re=0, when the inclination angle is low (γ=20°) iso-surfaces of temperature and concentration keep a similar appearance

which the case of γ=0° which is characterized by a vertical stratification. By the increase of the inclination angle, these iso-surfaces become more distorted and the thermal and solutal gradient increase for γ=90°. The increasing of the inclination angle modifies the flow structure from two vortex to one cell for Re=100.

- Case 3: Re=150

When γ=30°, a small vortex appears in the upper part of the cavity (figure 13). The other vortex, which already appears for γ=0°, still in the same position close to the moved cold wall and this for the two inclination angle γ=30° and 45°. By increasing γ, the small vortex disappears progressively (γ=60°) and the flow becomes mono-cellular for γ=75° and 90°. For (γ=90°), streamlines are closer to the cold moving wall with a little stretch to the top corner of it.

Figures 14 and 15, present the iso-surfaces of temperature and concentration for Re=150 and different inclination angles. The vertical stratification which appears for the vertical cavity is largely affected by the inclination angle for this case of study. In fact, when the inclination angle reaches the value of 30°, the iso-surfaces are more deformed especially in the upper part of the cavity. For γ=60° a mushroom form began to appear and becomes more developed for γ=90°.

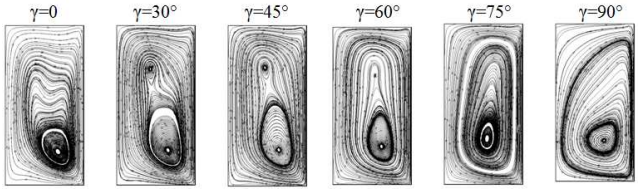

Figure 13. *Velocity vector projection in the XY-plan for Re=150 and different γ.*

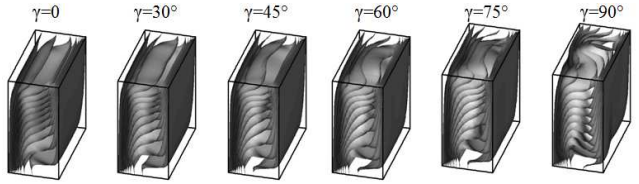

Figure 14. *Iso-surfaces of concentrations of temperature for Re=150 and different (γ).*

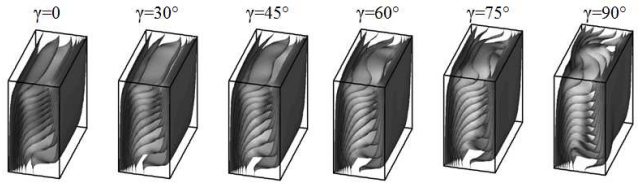

Figure 15*. Iso-surfaces of concentrations for Re=150 and different (γ).*

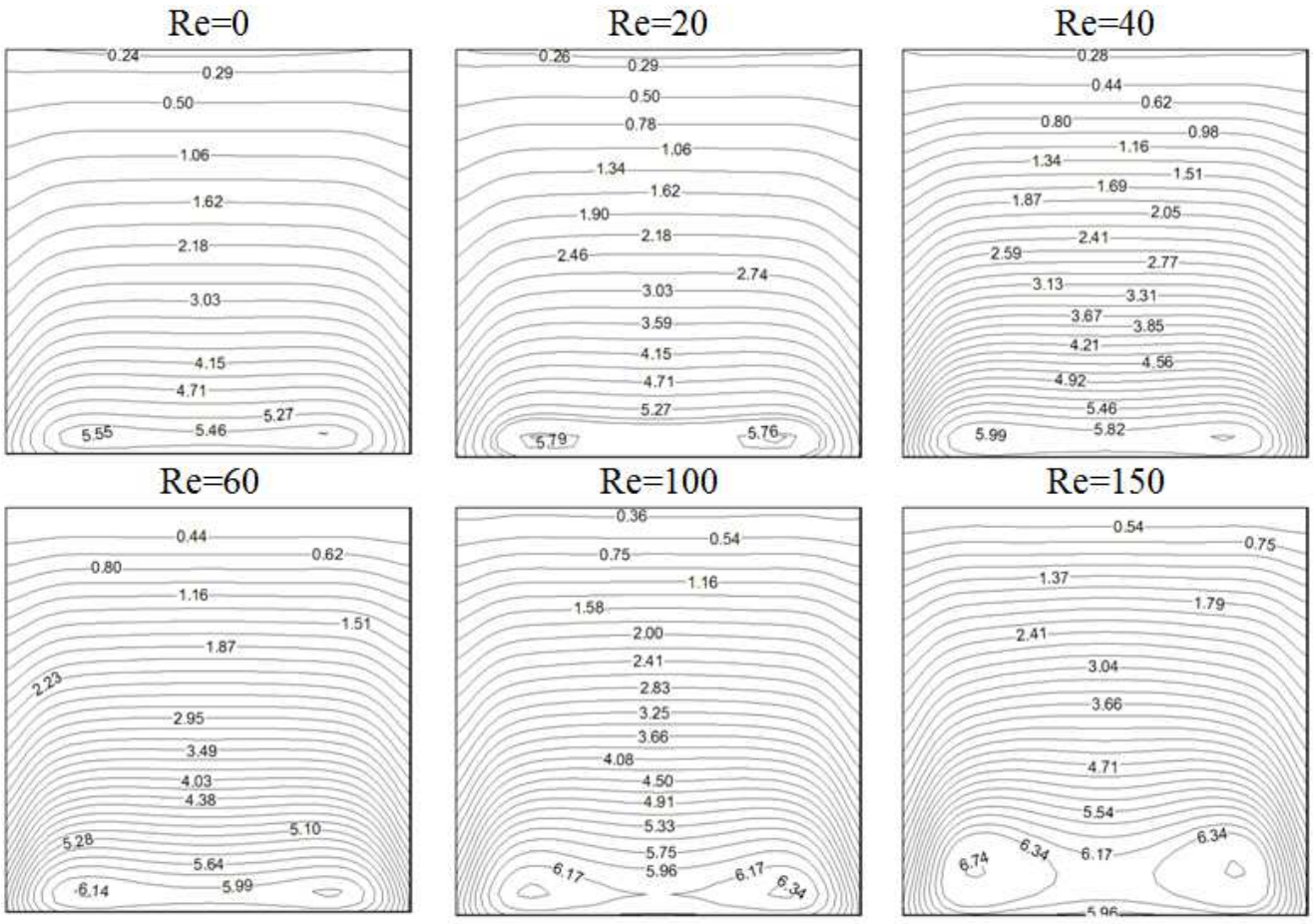

Figure 16. *Local Nusselt Number at the hot wall for γ=0 and different Re.*

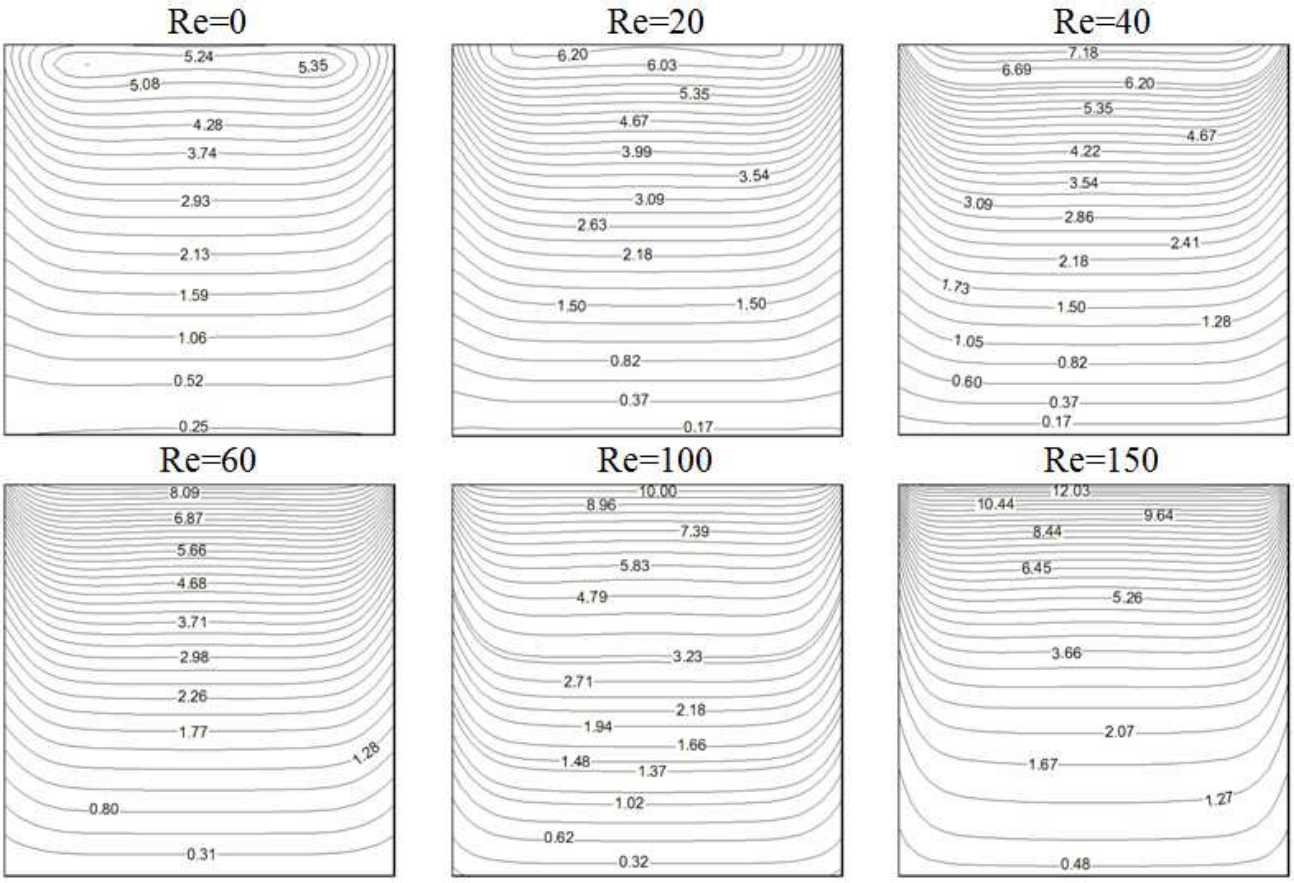

Figure 17. *Local Nusselt Number at the cold wall for γ=0 and different Re.*

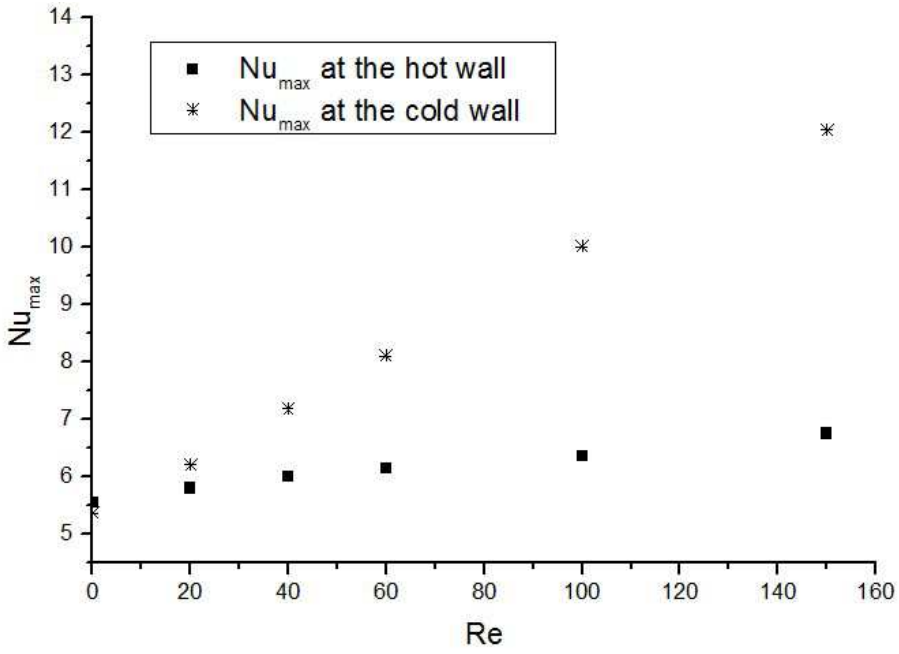

Figure 18. *Maximum of Nusselt numbers for different Re numbers.*

5.3. Study of Heat Transfer

This part is interested to study the effect of the variation of Reynolds numbers on the heat transfer distribution at hot and cold walls for a vertical cavity. Figures 16 and 17, present the Nusselt number contours respectively at the hot fixed wall and the cold moving wall for different Re. First of all, accelerating the cold wall induces an increase in values of the Nusselt number. Furthermore, near the active walls a three-dimensional character is visible by the deviation of the local

Nusselt number contours. The increase of Re induces a large modifications especially at the boundary.

When the cavity is vertical and the Re=0, local Nusselt number at the two vertical sides are asymmetric. When the cold wall is moved, contours of Nusselt numbers at the moving wall are modified. When the Re increases, contours at the cold wall, are more dispersed and are opened. However at the hot fixed wall, same behaviors as initial is kept and maximum appears near the down part and it is localized at a punctual region. These maximum contours levels are similar to two symmetric eyes which are intensified by the increase of Re values. The maximum value of Nu riches 6.74 for Re=150 however it is equal to 5.55 when Re=0 (up 17.65%).

For the behavior of the Nusselt numbers at the cold moved wall, a great increase of Nu values are detected relative to the increase of the Re numbers. In fact, this increase is equal to 55.52% from Re=0 to Re=150 (figure 18).

6. Conclusion

In this paper we studied numerically the three-dimensional double diffusive natural convection in a solar distiller with a moving cold wall. The Rayleigh number is fixed at Ra=10^5, Pr=0.7, Le=0.85, N=0.85 and the effects of Reynolds number is studied for opposed temperature and concentration gradients. The major results found in this study are:

- When the cavity is vertical we find that the movement of the cold wall induces an acceleration of heat and mass transfer and the heat and mass distribution throughout the cavity became more homogeneous.
- When the cavity is inclined, we note that the increasing of the inclination angle modifies the flow structure from two vortex to one cell when Re=100. Also, when the Re=150, we note that for an inclination angle equal to γ=60° a mushroom form began to appear and becomes more developed for γ=90°.
- The increase of the Nusselt number at the cold moved wall improves the condensation however its increase at the hot fixed wall improves the evaporation.

Nomenclature

Ay, Az	aspect ratios at Ay=H/W and Az =L/W
C	dimensionless species concentration
C'_h	high species concentration
C'_l	low species concentration
D	species diffusivity
Gr	Grashof number
H	cavity height
L	cavity side
Le	Lewis number
N	buoyancy ratio
$\overline{Nu}$	Average Nusselt Number
Pr	Prandtl number
Ra	Rayleigh number
Re	Reynolds number
Ri	Richardson number
Sh	Sherwood Number
t	dimensionless time (=$t'.\alpha / l^2$)
T	dimensionless temperature
T'_c	cold temperature
T'_h	hot temperature
$\vec{u}$	dimensionless velocity vector (=$\vec{u}.l / \alpha$)
W	enclosure width
Greek symbols	
α	thermal diffusivity
β_T	coefficient of thermal expansion
β_C	coefficient of compositional expansion
γ	inclination angle of the cavity
μ	dynamic viscosity
ν	kinematic viscosity.
υ_0	characteristic speed of fluid (=α / l)
ϕ'	dissipation function
$\vec{\psi}$	dimensionless vector potential ($\vec{\psi}' / \alpha$)
$\vec{\omega}$	dimensionless vorticity (=$\vec{\omega}'.\alpha / l^2$)
Subscripts	
c	cold
h	hot
m	mean
x, y, z	cartesian coordinates
Superscript	
’	dimensional variable

References

[1] D. Gobin and R. Bennacer, Cooperating thermosolutal convection in enclosures II: Heat transfer and flow structure. International Journal of Heat and Mass Transfer 39 (1996), 2683-2697.

[2] J. W. Lee and J. M. Hyun, Double-diffusive convection in a rectangle with opposing horizontal temperature and concentration gradients. International Journal of Heat and Mass Transfer 33 (1990), 1619-1632.

[3] J. M. Hyun and J. W. Lee, Double-diffusive convection in a rectangle with cooperating horizontal gradients of temperature and concentration. International Journal of Heat and Mass Transfer 33 (1990), 1605-1617.

[4] M. M. Naim (1987), Solar desalination spirally-wound module, Alternative Energy Sources VIII, T. N. Veziroglu, Ed., Hemisphere Publishing, 571-580.

[5] B. Bouchekima, Bernard Gros, Ramdane Ouahes and Mostefa Diboun, Theoretical study and practical application of the capillary film solar distiller, Renewable Energy 16 (1999), 795-799.

[6] B. Bouchekima, Bernard Gros, RamdaneOuahes and Mostefa Diboun, Etude théorique et application pratique du distillateur solaire à film capillaire, Int. J. Therm. Sci. 39 (2000), 442–459.

[7] B. Bouchekima, A small solar desalination plant for the production of drinking water in remote arid areas of southern Algeria, Desalination 159 (2003), 197-204.

[8] L. Ben Snoussi, R. Chouikh and A. Guizani, Numerical study of the natural convection flow resulting from the combined buoyancy effects of thermal and mass diffusion in a cavity with differentially heated side walls, Desalination, vol 182 (2005), 143–150.

[9] K. Sampathkumar, T. V. Arjunanb, P. Pitchandia and P. Senthilkumarc, Active solar distillation-A detailed review, Renewable and Sustainable Energy Reviews Volume 14, Issue 6 (August 2010), 1503-1526.

[10] A. Bergeon and E. Knobloch, Natural double diffusive convection in three-dimensional enclosures, Physics of fluids 14 (2002) 3233-3252.

[11] I. Sezai and A. A. Mohamad, Double diffusive convection in a cubic enclosure with opposing temperature and concentration gradients. Physics of fluids 12 (2000) 2210-2223.

[12] A. Abidi, L. Kolsi, M. N. Borjini, H. Ben Aissia and M. J. Safi, Effect of heat and mass transfer through diffusive walls on three-dimensional double-diffusive natural convection, Numerical Heat Transfer, Part A, vol 53 (2008), 1357–1376.

[13] K. Ghachem, L. Kolsi, C. Mâatki, A. K Hussein, M. N Borjini, Numerical simulation of three-dimensional double diffusive free convection flow and irreversibility studies in a solar distiller, International Communication of Heat and Mass Transfer 39 (2012), 869-876.

[14] M. K. Moallemi, K. S. Jang, Prandtl number effects on laminar mixed convection heat transfer in a lid-driven cavity, International Journal of Heat and Mass Transfer 35 (1992), 1881–1892.

[15] M. A. R. Sharif, Laminar mixed convection in shallow inclined driven cavities with hot moving lid on top and cooled from bottom, Applied Thermal Engineering 27 (2007), 1036–1042.

[16] K. M. Khanafer, A. M. Al-Amiri and I. Pop, Numerical simulation of unsteady mixed convection in a driven cavity using an externally sliding lid, European Journal of Mechanics - B/Fluids (2007), 669–687.

[17] H. F. Oztop, C. Sun and B. Yu, Conjugate-mixed convection heat transfer in a lid driven enclosure with thick bottom wall, International Communications in Heat and Mass Transfer 35 (2008), 779-785.

[18] M. A. Waheed, Mixed convective heat transfer in rectangular enclosures driven by a continuously moving horizontal plate, Journal of Heat and Mass Transfer 52 (2009), 5055–5063.

[19] V. Sivakumar, S. Sivasankaran, P. Prakash, J. Lee, Effect of heating location and size on mixed convection in lid-driven cavities, Computers & Mathematics with Applications 59 (2010), 3053–3065.

[20] T. S. Cheng, Characteristic of mixed convection heat transfer in a lid-driven square cavity with various Richardson and Prandtl numbers, International Journal of Thermal Science 50 (2011) 197–205.

[21] W. I Akand., A. R. S. Muhammad, E. S. Carlson, Mixed convection in a lid driven square cavity with an isothermally heated square blockage inside, International Journal of Heat and Mass Transfer 55 (2012), 5244–5255.

[22] I. Hajri, A. Omri and S. Ben Nasrallah, A numerical model for the simulation of double-diffusive natural convection in a triangular cavity using equal order and control volume based on the finite element method, Desalination 206 (2007), 579–588.

[23] R. Alvarado-Juárez, G. Álvarez, J. Xamán, I. Hernández-López, Numerical study of conjugate heat and mass transfer in a solar still device, Desalination 325 (2013), 84–94.

[24] A. A. Mohamad, R. Viskanta, Flow Structures and Heat Transfer in a Lid-Driven Cavity Filled with Liquid Gallium and Heated from Below, Experimental Thermal and Fluid Science 9 (1994), 309-319.

[25] N. Ouertatani, N. Ben Cheikh, B. Ben Beyaa, T. Lili, Antonio Campo, Mixed convection in a double lid-driven cubic cavity, International Journal of thermal Sciences 48 (2009), 1265–1272.

[26] L. Kolsi, H. F. Oztop, M. N. Borjini and K. Al-Salem, Second law analysis in a three dimensional lid-driven cavity, International Communication of Heat and Mass Transfer 38 (2011), 1376–1383.

[27] T. Nishimura, M. Wakamatsu, A. M. Morega, Oscillatory double diffusive convection in a rectangular enclosure with combined horizontal temperature and concentration gradients, Int. J. Heat Mass Transfer 41(1998), 1601-1611.

[28] A. J. Chamkha, H. Al-Naser, Hydromagnetic double-diffuse convection in a rectangular enclosure with opposing temperature and concentration gradients, Int. J. Heat Mass Transfer 45 (2002) 2465–2483.

[29] Kai-Long Hsiao, Heat and Mass Mixed Convection for MHD Viscoelastic Fluid Past a Stretching Sheet with Ohmic Dissipation, July 2010, Communications in Nonlinear Science and Numerical Simulation, 15 (2010) 1803–1812, ISSN: 1007-5704.

[30] I-Hua Lin, Kai-Long Hsiao, Food Extrusion Energy Conversion Conjugate Ohmic Heat and Mass Transfer for Stagnation Non-Newtonian Fluid flow with Physical Multimedia Features, American Journal of Heat and Mass Transfer, (2015) Vol. 2 No. 3 pp. 127-145 doi: 10.7726/ajhmt.2015.1009.